

Role of ionized nitrogen species in the optical and structural properties of GaInNAs/GaAs quantum wells grown by plasma-assisted molecular beam epitaxy

J. Miguel-Sánchez^{a)} and A. Guzmán

Institute for Systems Based on Optoelectronics and Microtechnology (ISOM) and Departamento de Ingeniería Electrónica, Universidad Politécnica de Madrid, E.T.S.I. Telecomunicación, Ciudad Universitaria s/n, 28040 Madrid, Spain

U. Jahn and A. Trampert

Paul-Drude-Institut für Festkörperelektronik, Hausvogteiplatz 5-7, 10117 Berlin, Germany

J. M. Ulloa

Institute for Systems Based on Optoelectronics and Microtechnology (ISOM) and Departamento de Ingeniería Electrónica, Universidad Politécnica de Madrid, E.T.S.I. Telecomunicación, Ciudad Universitaria s/n, 28040 Madrid, Spain

E. Muñoz and A. Hierro

Institute for Systems Based on Optoelectronics and Microtechnology (ISOM) and Departamento de Ingeniería Electrónica, Universidad Politécnica de Madrid, E.T.S.I. Telecomunicación, Ciudad Universitaria s/n, 28040 Madrid, Spain

(Received 14 December 2006; accepted 19 March 2007; published online 25 May 2007)

We report on the impact of the nitrogen ion density on the structural and optical properties of GaInNAs quantum wells (QWs) grown by molecular beam epitaxy. The optical emission is strongly increased when the nitrogen ion density is reduced, as we found from photoluminescence experiments. Cathodoluminescence mappings of QWs grown under different ion densities are compared, showing a stronger modulation depth, and thus a higher structural disorder when a higher ion density was present during the growth. Atomic force microscopy measurements of equivalent epilayers showed that ions cause an important structural disorder of the layers. A nearly double root-mean-square roughness is observed when the density of ions is not reduced by external magnetic fields. Additionally, results of transmission electron microscopy measurements of buried GaInNAs QWs are presented, showing that lateral compositional fluctuations of In and N are suppressed when the QWs are protected from the ions. Finally, we find that QWs exposed to higher ion densities during the growth show deeper carrier localization levels and higher delocalization temperatures. These results provide clear evidence that the density of nitrogen ions present in the chamber during the epitaxial growth of GaInNAs QWs directly limits both the structural and optical properties. © 2007 American Institute of Physics. [DOI: [10.1063/1.2733740](https://doi.org/10.1063/1.2733740)]

I. INTRODUCTION

In recent years much work has been devoted to understanding the properties of GaInNAs, due to its interesting characteristics for the development of optoelectronic devices, such as semiconductor light emitting diodes laser diodes (LDs) for telecommunication applications.¹ The possibility of growing virtually lattice-matched Al(Ga)As/GaAs Bragg reflectors, the strong reduction of its band gap with the addition of low nitrogen content, and a strong electron confinement,¹ make the GaInNAs material a good candidate to substitute GaInAsP based devices with high performance GaInNAs vertical cavity surface emitting lasers and edge-emitting LDs.²⁻⁵

But it is also widely reported in the literature, that the addition of small concentrations of N (typically less than 4%) to the InGaAs layers causes a strong reduction in the optical quality of the QWs, caused by the formation of non-

radiative recombination centers; mainly due to Ga vacancies,⁶ interstitial incorporation of N,⁷ nitrogen dimers in the lattice,⁸ and damage created during growth caused by N ionized species.⁹⁻¹³

The creation of the first two defects is related with growth dynamics and it can be controlled by the optimization of growth conditions. We focus here on the effect of the ionized nitrogen species.

To incorporate N to the samples, atomic N is needed. The usual method to obtain this free N atom in solid source molecular beam epitaxy (MBE) systems is to create a plasma from ultrapure N₂. Several species coexist in this plasmas: electrons, atomic nitrogen, diatomic nitrogen, and ionized nitrogen species.^{10,11} The ratio of this ionized species to the atomic nitrogen produced by a N plasma is called the ionization factor. The lower this ionization factor, the better the quality of a plasma used for epitaxial growth. As electron cyclotron resonance plasma sources show a higher ionization factor¹⁴ the most extended sources for epitaxial growth are radio frequency (rf) plasmas. The presence of these N₂⁺ ions

^{a)}Electronic mail: jmiguel@die.upm.es

in the chamber can be detected either optically, observing the transition $N_2(B^2\Sigma_u^+)$ to $N_2(X^2\Sigma_g^+)$ at 391.4 nm (Refs. 10 and 11) or electrically, as in our case, by using a modified Langmuir probe method,^{12,13} placed at the position of the sample.

We study in this work the effect of these N ionized species on the optical and structural properties of GaInNAs quantum wells (QWs) by varying the amount of ions that impinge onto the sample by using magnetic deflection. Atomic force microscopy (AFM) and transmission electron microscopy (TEM) measurements show the presence of structural damage caused by ions during growth. This disorder is correlated with the optical properties of the samples studied by cathodoluminescence (CL) and photoluminescence (PL) measurements. We show that the N ion concentration during growth is a key parameter that strongly affects the morphology, the optical emission, and the carrier localization in the GaInNAs QWs. This fact should be taken into account when comparing samples containing different N concentrations grown under different plasma conditions or from different MBE systems.

II. EXPERIMENTAL SETUP

The samples were grown by solid source molecular beam epitaxy, using a nitrogen rf plasma source. The growth was continuously monitored and controlled by *in situ* reflection high-energy electron diffraction (RHEED). The indium content was calibrated by InGaAs RHEED oscillations. Details of the growth parameters were reported elsewhere.¹³ The amount of ions impinging onto the surface was varied by applying a magnetic field perpendicular to the flow of the species from the plasma source to the sample. This was performed by placing a 0.2 T static magnet under an extension tube joining the source and the chamber. A strong reduction of the ion density impinging onto the sample was achieved, as measured by the modified Langmuir probe method.^{12,13,15}

AFM measurements were carried out in a Digital Instruments MMAFM-2 microscope after carefully cleaning the surface. The samples for TEM measurements were prepared in two perpendicular projections by mechanical polishing and grinding. Following this step, a 3.5 kV Ar^+ -ion milling was performed to achieve electron transparency. The TEM analysis was done in a JEOL 3010 microscope, equipped with a GATAN slow scan charge coupled device camera.

The PL emission was dispersed by a 1 m monochromator and detected by a cooled Ge detector. The 488 nm spectral line of an Ar^+ laser was used as the excitation source. For PL experiments at different temperatures, the samples were cooled down on a compressed He cryostat system.

The CL line profiles and micrographs presented in this work were recorded at a sample temperature of 12 K in a scanning electron microscope (SEM) equipped with a monochromator and integrated detector for the near infrared as well as with a He cooling stage system.

III. PHOTOLUMINESCENCE ANALYSIS

To study the effects of the density of ions present during growth in the chamber, on the optical properties

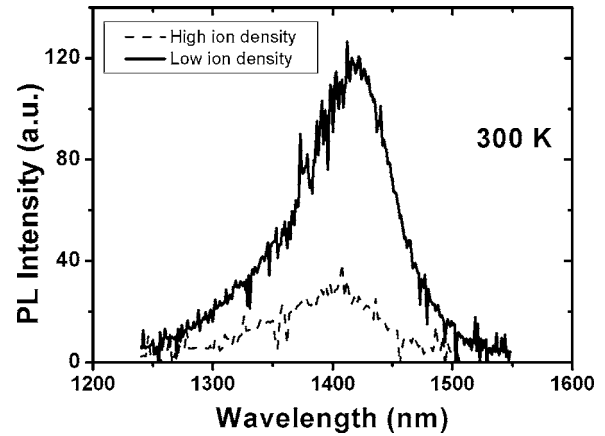


FIG. 1. Room temperature PL spectra of the GaInNAs QWs grown with high (dashed solid line) and low (black solid line) ion densities. The latter shows an improvement of PL intensity by a factor of 4.

of the GaInNAs QWs a set of two equivalent single QW samples were grown, consisting of a 7 nm thick $Ga_{0.7}In_{0.3}N_{0.017}As_{0.983}$ QW under a 100 nm thick GaAs barrier layer. The first QW was grown under the usual density of ions generated by the rf plasma source, while this ion density was strongly reduced during the growth of the second sample by means of the application of a magnetic field. The transition from the $c(4 \times 4)$ to (2×4) RHEED surface reconstructions patterns were chosen as temperature reference to ensure that the growth temperature was the same for both samples. We found no appreciable differences between both samples in the GaInNAs RHEED patterns: both were streaky patterns throughout the growth, indicating that no three-dimensional growth of the material occurred. The room temperature photoluminescence spectra of these QWs are plotted in Fig. 1. As seen in the figure, and as stated in other works in the literature,^{12,13,15} the sample grown with the reduced ion density (black solid line) shows a higher optical quality, with a narrower [10 meV lower full width at half maximum (FWHM)] and a four times more intense PL emission peak than the QW grown with the usual ion density (gray solid line). For this comparison, these measurements were performed at room temperature, where localization effects are negligible for both samples, as we will see in the following sections.

IV. CATHODOLUMINESCENCE ANALYSIS

Although CL measurements at these wavelengths (1.3 and 1.5 μm) are powerful tools to analyze the GaInNAs material, few works have been presented on this topic.^{16,17} This CL technique combined with TEM, AFM, and PL measurements provide us with a deeper understanding of the optical and structural properties of the GaInNAs quantum wells.

The CL mapping using a value of the detection energy, which corresponds to the high energy flank (at the higher energy of the FWHM) of the CL emission, was measured at 12 K. These mappings are shown in Fig. 2. Note that the dark spot of the CL mapping of the high ion density sample [Fig. 2(a)] is due to a dust particle, as evidenced by its presence in the SEM image. As observed in the mappings, the

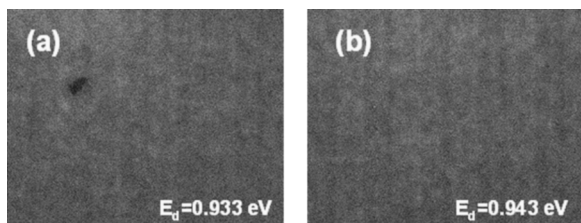


FIG. 2. Low temperature (12 K) CL mappings of the GaInNAs QWs grown with a high (a) and low (b) ion densities. The detection energies were 0.933 and 0.943 eV, respectively, which corresponds to the high-energy flank of the respective CL spectra.

emission appears quite homogenous, but some dot-like granularity is observed in both images. To quantitatively analyze the lateral distribution of the CL emission, we performed line scans at 12 K. These line scans consist of the measurement of the CL intensity along a given direction at a fixed detection energy. For the line scans shown in Fig. 3, this energy is the same one as used for the CL mappings shown in the previous figure (detection energies were 0.933 and 0.943 eV for the high and low ion density QWs, respectively). As seen in this figure, the CL intensity of the low ion density sample is 2–3 times higher than the one of the QW grown with high ion density, which is consistent with the previous PL measurements. Additionally, these line scans clearly reveal the fluctuations with bright spots of around $4 \mu\text{m}$ diameter as mentioned earlier. Lateral variations of the CL intensity, have already been previously observed in GaInNAs QWs by Kitatani *et al.*¹⁶ with similar “dot” sizes. To compare both line scans we used the root-mean-square (rms) modulation depth (MD), defined as the root-mean-square of the standard deviation of the measured intensity, divided by the mean intensity, that is: $\text{MD}_{\text{rms}} \equiv \sqrt{\langle(\delta I)^2\rangle}/\langle I \rangle$.¹⁷ We can now directly compare both QWs with this technique. The calculations yielded MDs of 17.3% and 9.7% for the samples with high and low ion densities, respectively. This MD reveals the underlying disorder of the quantum well.¹⁸ Thus, we can tentatively conclude that the higher intensity of the GaInNAs QWs grown with reduced nitrogen ion density could be related to a better structural quality of these layers compared to those of the QWs grown with the usual nitrogen ion density.

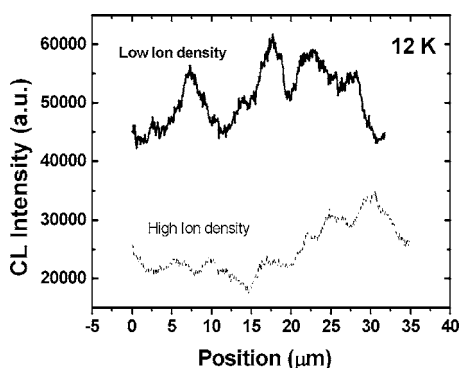


FIG. 3. Line scans of the low temperature (12 K) CL intensity of the GaInNAs QWs grown with a high (dashed line) and low (solid line) ion density. The detection energies were 0.933 and 0.943 eV, respectively.

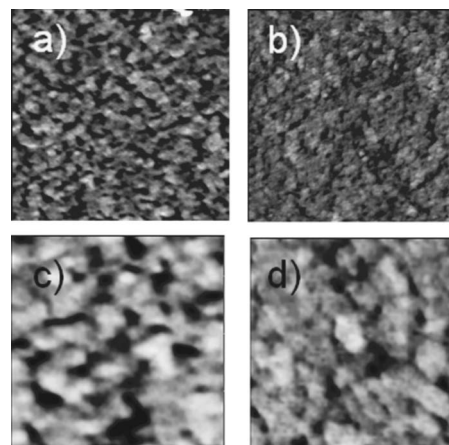


FIG. 4. AFM images of the GaInNAs epilayers, grown with a high [(a),(c)] and a low [(b),(d)] ion density. (a) and (b) scans are $500 \text{ nm} \times 500 \text{ nm}$ with a vertical scale of 3 nm. (c) and (d) scans are $180 \text{ nm} \times 180 \text{ nm}$ with a vertical scale of 5 nm.

To confirm this picture AFM and TEM analysis were performed on GaInNAs epilayers and QWs, as explained in the following sections.

V. STRUCTURAL PROPERTIES

As seen in the previous section and as stated in previous works, the deterioration of the structural properties of the GaInNAs QWs is linked to a higher density of nitrogen ions during growth.^{9,13} However, in these reports, this deterioration was indirectly deduced from the fact that a lower optimum rapid thermal annealing temperature was needed when a low ion density was used, indicating a higher structural quality.¹⁹ Here, AFM and TEM techniques were used to directly determine the structural properties of epilayers and embedded QWs, respectively, grown under different amounts of nitrogen ions.

A. Atomic force microscopy investigations

To study the morphology of the GaInNAs layers with AFM, 7 nm thick epilayers (with high and low ion densities) were grown under exactly the same growth conditions of the previously described QWs. The nitrogen plasma was switched off and nitrogen flow was stopped immediately after the completion of the growth of the epilayer. Figures 4(a) and 4(c) show the surface of the GaInNAs epilayer grown without the magnetic field, thus with a “high” density of N ions impinging on it. As observed in this figure, a high surface modulation is found and the presence of tens of nanometers-sized “holes” can be recognized. The creation of such holes has already been reported by other groups.²⁰ A 0.53 nm rms roughness was calculated for this surface. The depth of these holes was found to correspond to more than 10 ML in some cases. Figure 5(a) shows typical cross-sectional profiles of both epilayers where the fluctuations are clearly observed. Undulations of similar dimensions of the upper interface of the QW were previously detected in TEM measurements of GaInNAs QWs.^{19,21,22} On the other hand, the surface of the epilayer grown with the reduced ion density is a much more compact layer [Figs. 4(b) and 4(d)], with

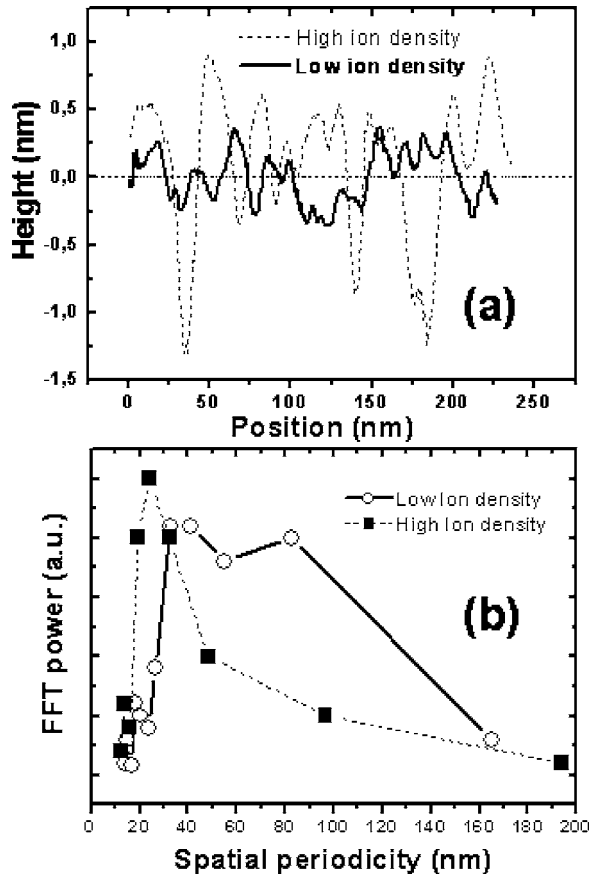


FIG. 5. (a) Surface line profiles of the GaInNAs epilayers, measured by AFM. The dashed (solid) line shows the epilayer grown with a high (low) ion density. (b) Fast-Fourier transform of the average of several cross-sectional profiles of the epilayers grown with a high (filled squares) and a low (hollow circles) ion density. Lines are interpolations between data points.

a rms roughness of only 0.35 nm. The measurements of the cross-sectional profile of this layer [gray solid line in Fig. 5(a)] reveal steps of only one to up to 4 ML. Additionally, we can statistically study the fluctuations of both surfaces to obtain information about the periodicity of these undulations. In Fig. 5(b), we show the fast-Fourier transform (FFT) of the averages of the cross-sectional profiles of both surfaces. The solid lines are interpolations between data points. For the sample with high ion density (black squares), the FFT high power components concentrate mainly between 20 and 50 nm, which indicates a distinct periodicity of the features (holes) in the surface damaged by the ions. On the contrary, a broadband with no clear periodicity is obtained for the GaInNAs surface grown with the reduced ion density (hollow circles), thus indicating a higher structural quality and a flatter surface, showing no clear periodicity. Thus, we see from this analysis a strong reduction of surface roughness when the density of ions is significantly reduced.

B. Transmission electron microscope Investigations

The GaInNAs structural properties are very sensitive to growth parameters,²³ and in particular, to growth temperature.²⁴ This temperature must be very low (compared to the optimum growth temperature of InGaAs) to avoid the

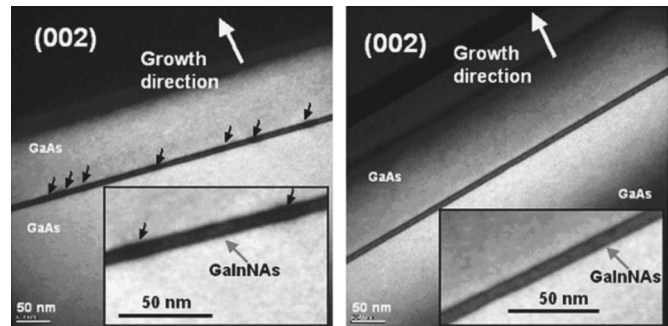


FIG. 6. Cross-sectional TEM image of the GaInNAs QWs grown without (a) and with (b) a deflecting magnetic field to reduce ion density, taken with diffraction vector $g(002)$, which is sensitive to the composition of the layer. The insets show in more detail the microstructure of the QWs. The black and white arrows indicate the compositional fluctuations and the growth direction, respectively.

Stanski-Krastanov, i. e., a three-dimensional (3D) growth mode or the creation of surface undulations on the upper interface of the QWs. Additionally, in many cases an intermediate step between the two-dimensional (2D) and the 3D growth mode has been reported, consisting of the growth of completely 2D QWs but with lateral compositional modulation of In and N, with typical modulation periods between 10 and 50 nm.^{21,22,25} These compositional modulations are related to the presence of N during growth,^{26,27} since these fluctuations were not observed in the InGaAs material. Here we show that these compositional fluctuations are enhanced by the presence of ions during growth. For this purpose, we studied two equivalent QWs with the same thickness and composition, but grown with and without the application of the deflecting magnetic field, by TEM as the epilayers studied above by AFM. Figures 6(a) and 6(b) show cross-sectional TEM images of these GaInNAs QWs, taken with a diffraction vector $g=002$, which is sensitive to the composition of the alloy.^{21,25} As observed in this figure, very small thickness fluctuations were found, indicating a pure 2D growth mode during the epitaxy of the layers. This is consistent with the earlier mentioned RHEED observations. A very slight modulation can be established in the upper interface of the QW grown under a high ion density [cf. Fig. 6(a)]. In addition to this, some compositional modulations along the QW are observed. The alternating lateral contrast is mainly due to variations in the In and N mole fraction.^{21,25–27} These fluctuations in the composition are spaced between 20 and 100 nm, as observed in Fig. 6(a). This fluctuation periodicity is in the same order of magnitude of the surface periodicity found for the epilayer grown under the same conditions, as exposed earlier in the AFM measurements. In Fig. 6(b), the QW grown with the reduced ion density does not show any thickness fluctuation, thus indicating a perfect 2D growth mode. Additionally, compositional fluctuations are also not found along the well. This lateral composition modulation is reported in the literature to be caused by the simultaneous incorporation of In and N in the QWs. During the epitaxial growth, the alloy formation is driven by the minimization of the quaternary free energy, including local strain and cohesive bond energy terms. In the GaInNAs material, the growth is mainly driven by maximizing the cohe-

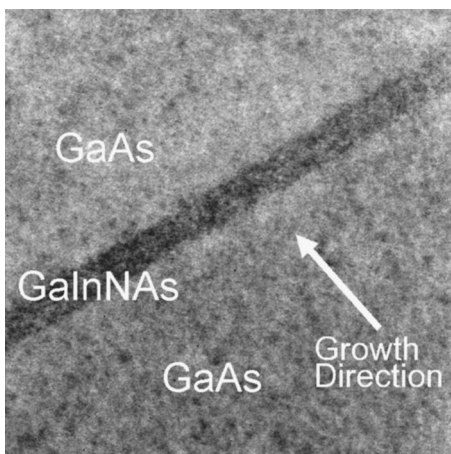


FIG. 7. High-resolution TEM picture of the GaInNAs QW grown with reduced ion density. Upper and lower interfaces are indistinguishable.

sive bond energy. For this reason, lateral compositional fluctuations are formed along the QW.^{26,27} In the case under study, we clearly observe that for the GaInNAs/GaAs QWs grown under the same conditions, these fluctuations are strongly reduced, if the ion density is decreased. The energetic nitrogen ions impinging onto the near surface transition layer enhance the formation of the high energy Ga-N and In-As bonds and therefore cause the formation of composition modulations along the QW. This picture is consistent with previous experiments indicating a reduced annealing-induced blueshift of the PL from GaInNAs QWs when a magnetic field was applied for the deflection of ions during the growth,^{9,13} since the observed blueshift is mainly caused by bond reorganization within the QW.^{28,29} The corresponding bond rearrangement involves a breaking of Ga-N bonds and the creation of new In-N bonds, which leads to an increase of the energy band gap for the GaInNAs material.^{28–30}

With this experiment we have direct evidence of the strong correlation of the density of ions impinging onto the surface during growth and the compositional modulation of GaInNAs QWs: When this density is strongly reduced by the application of a deflecting magnetic field the lateral composition modulation is suppressed. Figure 7 shows the high-resolution TEM (HRTEM) cross-sectional image of the sample with reduced ion density. Here we can observe the smoothness of the interfaces of the QW, showing thickness fluctuations of only few monolayers. Both the upper and the lower interfaces show the same structural quality, being indistinguishable in our TEM observations.

VI. EFFECT OF IONS ON CARRIER LOCALIZATION

The addition of a small amount of nitrogen leads to a strong shrinkage of the band gap of GaInNAs QWs.¹ Moreover, a high density of localized states appear below the band edge.^{31,32} These can be detected by measuring the temperature (T) dependence of the PL peak energy resulting in the so-called s-shaped behavior.^{19,31,32} This is exactly what we obtained for both QWs under study, as shown in Fig. 8, where the T dependence of the PL peak energy of the low and high ion density samples is represented as hollow circles and black squares, respectively. The solid lines are β -spline

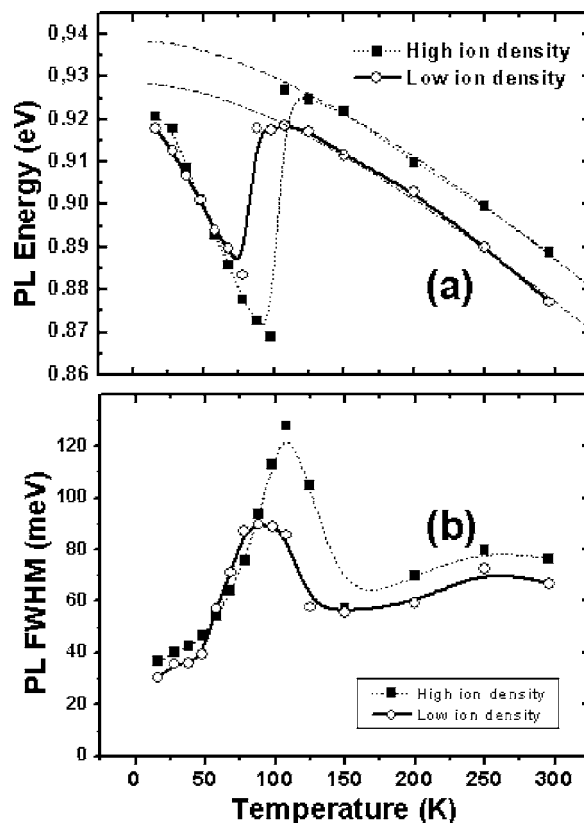


FIG. 8. (a) Temperature dependence of the PL peak energy for the sample grown with high (filled squares) and low (hollow circles) ion densities. Solid and dashed lines are β -spline interpolations drawn as a guide for the eye. Dash-dot lines are fittings to the experimental data using Varshni model. (b) Temperature dependence of the PL FWHM of the GaInNAs QWs with high (filled squares) and low (hollow circles) ion densities. Solid and dashed lines are interpolations drawn as a guide for the eye.

interpolations between the experimental data points serving as a guide for the eye. The dashed lines correspond to fittings to the Varshni model³³ for the temperature dependence of the gap energy, which was reported to be very accurate for GaInNAs QWs:³¹ $E(T) = E(0) - \alpha T^2 / (T + \beta)$, with $\alpha = 3.4 \times 10^{-4}$ eV K⁻¹, $\beta = 296$ K, and $E_{\text{high}}(0) = 938.5$ meV and $E^{\text{low}}(0) = 928.5$ meV for the high and low ion density QWs, respectively. At lower temperatures, the observed optical emission is mainly due to transitions from localized states. In this region, we observe that the transition energy decreases with increasing T . For T values reaching the delocalization temperature (T_{loc}), carriers are thermally activated and the population of the conduction band is increased. After the temperature exceeds T_{loc} , the optical emission is mainly due to transitions from the conduction band. As observed in Fig. 8, the agreement between the experimental data points and the Varshni model fitting is excellent for temperatures above 100 K for both samples where within this temperature range, localization effects are negligible. To estimate the value of T_{loc} different parameters can be studied.¹⁹ First, we can compare the temperature at which delocalization occurs. In the figure, it is clearly observed that the value of T_{loc} is lower for the QW grown with the reduced ion density ($T_{\text{loc}}^{\text{low}} \sim 80$ K) than for the high ion density sample ($T_{\text{loc}}^{\text{high}} \sim 100$ K), thus implying a larger localization energy for the latter. Another estimation of the localization energy is the difference be-

tween the observed emission energy, from the localized states and the simulated band gap energy. At T_{loc} , this energy is also much higher for the sample grown with higher ion density: $E_{\text{loc}}^{\text{low}}(77\text{ K})=35.2\text{ meV}$ vs $E_{\text{loc}}^{\text{high}}(100\text{ K})=59\text{ meV}$.

Further support for the correlation between carrier localization and the density of nitrogen ions during growth is given by the temperature dependence of the PL FWHM [Fig. 8(b)]. As the value of T_{loc} is approached, the PL starts to be composed by emissions from the localization centers (low energy) as well as from the band edge (high energy). This effect gives rise to a large broadening of the PL emission for T values around the delocalization temperature, which disappears at higher temperatures where the band edge emission is the only one that remains. Thus, the temperature, at which the PL FWHM exhibits a maximum, corresponds to T_{loc} [Fig. 8(b)]. Moreover, the PL FWHM of the high ion density QW remains larger even for higher temperatures, consistent with having a lower structural quality. The observation of this higher localization in the QWs grown with a higher ion concentration could be mainly due to the fact that these QWs show a stronger lateral compositional fluctuation (as shown in TEM observations) that yield a stronger localization in GaInNAs/GaAs system.³⁴

VII. CONCLUSIONS

We have observed a strong improvement of the PL intensity of GaInNAs QWs when a magnetic field is used to reduce the nitrogen ion density impinging onto the surface during the growth using plasma-assisted MBE. CL investigations showed uniform mappings with weak lateral inhomogeneities of the CL intensity. Detailed CL line scans showed fluctuations of the intensity along the well. A stronger CL modulation depth was found for samples grown with a higher ion density. We correlated this deeper modulation to a more disordered QW. AFM analysis of equivalent GaInNAs epilayers corroborated this picture, showing that the sample grown with the deflecting magnetic field was smoother as compared with the one grown without magnetic field. The epilayer grown under high ion concentration was much rougher and the analysis of this damaged surface revealed the presence of periodic features with spatial period between 20 and 50 nm. This fact was consistent with the TEM analysis, where lateral compositional fluctuations with a comparable period were found. The QW grown with a reduced ion density exhibits a perfectly smooth 2D QW with small variations of very few monolayers at the interfaces, as shown in HRTEM investigations. Finally, a study of the energy of the optical transition measured by PL at different temperatures revealed a stronger localization for the QWs grown under a higher ion density. Thus, we conclude that the ionization factor of the plasma source and the plasma conditions used for the growth of the GaInNAs QW is a source of degradation of the QW properties and should really be taken into account when comparing the optical (intensity, FWHM, localization energy) and structural properties (roughness, lateral compositional fluctuations) of those QWs grown under different rf nitrogen plasma conditions or in different growth chambers.

ACKNOWLEDGMENTS

The authors would like to thank M. Sari for his help in the preparation of some of the TEM specimens. This work has been partially supported by the Spanish Ministerio de Educación y Ciencia, Projects No. TEC2005–03694/MIC and No. NAN2004–09109-C04–02, Comunidad Autónoma de Madrid, Project No. S05051ESP-0200, and Acción Integrada HA2002–0004.

- ¹M. Kondow, K. Uomi, A. Niwa, T. Kitatani, S. Watahiki, and Y. Yazawa, *Jpn. J. Appl. Phys., Part 1* **35**, 1273 (1996).
- ²D. A. Livshits, A. Yu. Egorov, and H. Riechert, *Electron. Lett.* **36**, 1381 (2000).
- ³N. Tansu, N. J. Kirsch, and L. J. Mawst, *Appl. Phys. Lett.* **81**, 2523 (2002).
- ⁴C. S. Peng, T. Jouhti, P. Laukkanen, E.-M. Pavelescu, J. Konttinen, W. Li, and M. Pessa, *IEEE Photonics Technol. Lett.* **14**, 275 (2002).
- ⁵J. S. Harris, Jr., *J. Cryst. Growth* **278**, 3 (2005).
- ⁶W. Li, M. Pessa, T. Ahlgren, and J. Decker, *Appl. Phys. Lett.* **79**, 1094 (2001).
- ⁷S. G. Spruytte, M. C. Larson, W. Wampler, C. W. Coldern, H. E. Petersen, and J. S. Harris, *J. Cryst. Growth* **227–228**, 506 (2001).
- ⁸M. Ramsteiner, D. S. Jiang, J. S. Harris, and K. H. Ploog, *Appl. Phys. Lett.* **84**, 1859 (2004).
- ⁹Z. Pan, L. H. Li, W. Zhang, Y. W. Lin, R. H. Wu, and W. Ge, *Appl. Phys. Lett.* **77**, 1280 (2000).
- ¹⁰H. Carrère, A. Arnoult, A. Ricard, and E. Bedel-Pereira, *J. Cryst. Growth* **243**, 295 (2002).
- ¹¹H. Carrère, A. Arnoult, A. Ricard, X. Marie, Th. Amand, and E. Bedel-Pereira, *Solid-State Electron.* **47**, 419 (2003).
- ¹²J. Miguel-Sánchez, A. Guzmán, J. M. Ulloa, A. Hierro, and E. Muñoz, *IEE Proc.: Optoelectron.* **151**, 305 (2004).
- ¹³J. Miguel-Sánchez, A. Guzmán, J. M. Ulloa, A. Hierro, and E. Muñoz, *Appl. Phys. Lett.* **84**, 2524 (2004).
- ¹⁴M. R. Wertheimer and M. Moisan, *Pure Appl. Chem.* **66**, 1343 (1994).
- ¹⁵J. Miguel-Sánchez, A. Guzmán, J. M. Ulloa, A. Hierro, and E. Muñoz, *J. Cryst. Growth* **278**, 234 (2005).
- ¹⁶T. Kitatani, K. Nakahara, M. Kondow, K. Uomi, and T. Tanaka, *J. Cryst. Growth* **209**, 345 (2000).
- ¹⁷U. Jahn, S. Dhar, R. Hey, O. Brandt, J. Miguel-Sánchez, and A. Guzmán, *Phys. Rev. B* **73**, 125303 (2006).
- ¹⁸E. Runge, J. Menniger, U. Jahn, R. Hey, and H. T. Grahn, *Phys. Rev. B* **52**, 12207 (1995).
- ¹⁹A. Hierro *et al.*, *J. Appl. Phys.* **94**, 2319 (2003).
- ²⁰Y. Park, M. J. Cich, R. Zhao, P. Specht, H. Feick, and E. R. Weber, *Physica B* **308–310**, 98 (2001).
- ²¹A. Trampert, J.-M. Chauveau, K. H. Ploog, E. Tournié, and A. Guzmán, *J. Vac. Sci. Technol. B* **22**, 2195 (2004).
- ²²V. Grillo, M. Albrecht, T. Remmele, and H. P. Strunk, *J. Appl. Phys.* **90**, 3792 (2001).
- ²³H. F. Liu, S. Karirinne, C. S. Peng, T. Jouhti, J. Konttinen, and M. Pessa, *J. Cryst. Growth* **263**, 171 (2004).
- ²⁴M. O. Fischer, M. Reinhardt, and A. Forchel, *IEEE J. Sel. Top. Quantum Electron.* **7**, 149 (2001).
- ²⁵J.-M. Chauveau, A. Trampert, K. H. Ploog, M.-A. Pinault, and E. Tournié, *Appl. Phys. Lett.* **82**, 3451 (2003).
- ²⁶X. Kong, A. Trampert, E. Tournié, and K. H. Ploog, *Appl. Phys. Lett.* **87**, 171901 (2005).
- ²⁷X. Kong, A. Trampert, and K. H. Ploog, *Micron* **37**, 465 (2006).
- ²⁸S. Karirinne, E. M. Pavelescu, J. Konttinen, T. Jouhti, and M. Pessa, *New J. Phys.* **6**, 192 (2004).
- ²⁹K. Uno, M. Yamada, I. Tanaka, O. Ohtsuki, and T. Takizawa, *J. Cryst. Growth* **278**, 214 (2005).
- ³⁰K. Kim and A. Zunger, *Phys. Rev. Lett.* **86**, 2609 (2001).
- ³¹I. A. Buyanova, W. M. Chen, and C. W. Tu, *Semicond. Sci. Technol.* **17**, 815 (2002).
- ³²M.-A. Pinault and E. Tournié, *Appl. Phys. Lett.* **78**, 1562 (2001).
- ³³Y. P. Varshni, *Physica* **34**, 149 (1967).
- ³⁴J. M. Ulloa, A. Hierro, J. Miguel-Sánchez, A. Guzmán, J. M. Chauveau, A. Trampert, E. Tournié, and E. Calleja, *Semicond. Sci. Technol.* **21**, 1047 (2006).